

## Article

# Quaternization of Porous Cellulose Beads and Their Use for Removal of Humic Acid from Aqueous Medium

Kana Uchiyama <sup>1</sup>, Hiromichi Asamoto <sup>2</sup>, Hiroaki Minamisawa <sup>2</sup> and Kazunori Yamada <sup>3,\*</sup> 

<sup>1</sup> Major of Applied Molecular Chemistry, Graduate School of Industrial Technology, Nihon University, 1-2-1 Izumi-cho, Narashino 275-8575, Chiba, Japan

<sup>2</sup> Department of Basic Science, College of Industrial Technology, Nihon University, 2-11-1 Shin-ei, Narashino 275-8576, Chiba, Japan

<sup>3</sup> Department of Applied Molecular Chemistry, College of Industrial Technology, Nihon University, 1-2-1 Izumi-cho, Narashino 275-8575, Chiba, Japan

\* Correspondence: yamada.kazunori@nihon-u.ac.jp; Tel.: +81-47-474-2571

**Abstract:** Porous cellulose beads were quaternized with glycidyltrimethylammonium chloride (GTMAC) to explore a potential use of them as an adsorbent for removal of humic acid (HA) from aqueous medium. The introduction of quaternary ammonium groups was confirmed by FT-IR and XPS analysis. The content of introduced quaternary ammonium groups increased with an increase in the GTMAC concentration. The adsorption capacity increased with a decrease in the initial pH value and attained the maximum value at pH 3 and increased with an increase in the content of quaternary ammonium groups. The removal % increased with the dose of quaternized cellulose beads at both pH 3.0 and 6.0. The adsorption process obeyed the pseudo-second order kinetic model and exhibited a better fit to the Langmuir isotherm model, suggesting that the adsorption of HA is accomplished through the electrostatic interaction between a quaternary ammonium group introduced and a dissociated carboxy group of a HA molecule. The maximum adsorption capacity obtained in this study is comparable to or higher than those published by other articles. HA loaded was completely released to NaOH solutions at higher than 100 mM to regenerate the quaternized cellulose beads. The above-mentioned results clearly show that the quaternized cellulose beads prepared in this study can be used as a regenerable adsorbent with high capacity for removal of HA from aqueous medium.



**Citation:** Uchiyama, K.; Asamoto, H.; Minamisawa, H.; Yamada, K.

Quaternization of Porous Cellulose Beads and Their Use for Removal of Humic Acid from Aqueous Medium. *Physchem* **2023**, *3*, 61–76. <https://doi.org/10.3390/physchem3010005>

Academic Editor: Ramón G. Rubio

Received: 23 November 2022

Revised: 16 December 2022

Accepted: 4 January 2023

Published: 10 January 2023



**Copyright:** © 2023 by the authors. Licensee MDPI, Basel, Switzerland. This article is an open access article distributed under the terms and conditions of the Creative Commons Attribution (CC BY) license (<https://creativecommons.org/licenses/by/4.0/>).

**Keywords:** porous cellulose beads; quaternization; quaternary ammonium group; humic acid; adsorption; desorption

## 1. Introduction

Humic substances are formed through the chemical and biological humification of plants and through the biological activities of micro-organisms widely distributed in surface waters, sediments, and soils. Humic substances can be divided into three different components: fulvic acid, humic acid (HA), and humin based on the solubility [1,2]. Of them, HA is not soluble in water under acidic conditions (pH < 2) but is soluble at higher pH values. Although HA has different kinds of functional groups in structure, the most predominant are phenolic hydroxy and carboxy groups [3–5].

The presence of HA in natural waters causes undesirable color and taste and may also cause various environmental and health problems; HA serves as food for bacterial growth in water distribution systems. In addition, HA has the ability to bind a large range of metals and metalloids, such as Al(III), Pb(II), Ca(II), Mn(II), Mg(II), Fe(III), As(V) to form heteromolecular complexes. In the presence of chlorine and chloramine, which are added to disinfect water, disinfection byproducts, including trihalomethanes, haloacetic acids, and haloacetonitriles, can be generated through reactions with HA. These byproducts are potentially carcinogenic, although HA is harmful in itself [6,7]. As just described, the

presence of HA in water resources has been of major concerns in water supply and there is practical interest to remove HA in drinking water and other process waters.

Various removal methods of HA have been reported, such as chemical coagulation [8], membrane separation [9], oxidation [10,11], and adsorption [12]. Among these methods, adsorption is considered a promising method for removal of various pollutants from wastewater, owing to its simplicity, high removal efficiency, and low-cost. In adsorption methods, porous materials are widely used as an adsorbent matrix. Activated carbons produced from different kinds of agricultural materials have been prepared to be applied to the removal of HA in many articles [13–15]. However, their use is frequently limited because of disadvantages, such as high cost for chemical activation, slow adsorption rate, low adsorption capacity, and difficulty of regeneration.

Cellulose can be considered as a candidate as an alternative of activated carbon in the following viewpoints. Cellulose is the major component of plant cell walls and the most abundant polysaccharide in nature. The Cellulose chains consisting of repeated  $\beta$ -1,4 linked D-glucopyranose units can be present in ordered structure due to the absence of side chains or branched chains [16]. Although cellulose has a primary hydroxy (-OH) group at the C-6 position and two secondary hydroxy (-CH<sub>2</sub>OH) groups at the C-3 and C-4 positions in each anhydroglucose unit (AGU), it is insoluble in water and in common organic solvents due to strong inter- and intramolecular hydrogen-bonding interactions [17,18]. Cellulose exhibits above-mentioned unique physicochemical properties suitable for an adsorbent matrix and undertakes productive chemical functionalization through hydroxy groups. Therefore, many investigations have been published on widespread use of functionalized cellulose-based materials for removal of metallic and organic pollutants [9,19–22]. However, the investigation on the functionalization of cellulose materials and their application to water treatment is still a great challenge.

In this study, commercially available porous cellulose beads were functionalized with glycidyltrimethylammonium chloride (GTMAC) to introduce quaternary ammonium groups. The quaternization of the cellulose beads was confirmed by Fourier transform infrared (FT-IR) and X-ray photoelectron spectroscopy (XPS) analysis. The adsorption of HA on the quaternized cellulose beads was estimated by varying the experimental parameters, such as the initial pH value, the temperature, the content of quaternary ammonium groups, and the dose of quaternized cellulose beads, and then the adsorption behavior was characterized by the kinetic, isotherm, and equilibrium analysis. In addition, desorption of HA was also investigated for the practical use.

## 2. Materials and Methods

### 2.1. Chemicals

Porous cellulose beads, Viscop pearl-mini<sup>®</sup>, were purchased from Rengo Co., Ltd. (Osaka, Japan), which have the diameter of 0.3 mm, the bulk specific gravity of 0.2 g/mL, the water absorptivity of 3.5 g/10 mL, specific surface area of 10 m<sup>2</sup>/g, and the porosity of 87%. These data are nominal values from the manufacturer. GTMAC (80% aqueous solution) was purchased from Tokyo Chemical Industry Co., Ltd. (Tokyo, Japan). Other chemicals were used as received.

### 2.2. Quaternization of Cellulose Beads

A given amount of GTMAC was dissolved in a NaOH solution at 5 w/v% to give a volume of 50 mL. First, 5.0 g of porous cellulose beads were dispersed in a NaOH solution at 5 w/v% for 24 h. Then, the GTMAC solution was added to this mixture solution so as to make the concentration of 0.10 to 1.0 M and stirred for 0.5–4 h at 65 °C [23–25]. After the reaction, the porous cellulose beads isolated by decantation were thoroughly washed in the order of diluted HCl, water, and acetone, and then dried under reduced pressure.

### 2.3. Determination of Content of Quaternary Ammonium Groups

Under nitrogen atmosphere, 0.10–0.60 g of the quaternized cellulose beads were immersed in 10.0 mL of a HCl solution at 20.0 mM and the solutions were mildly stirred for 18–24 h. The aliquots taken from the supernatants were titrated with a NaOH solution at 10.0 mM in the presence of bromothymol blue used as an indicator. The content of quaternized ammonium groups per 1.0 g of dry quaternized cellulose beads was determined from the concentration difference in the HCl solution using Equation (1):

$$\text{content of quaternary ammonium groups (mmol/g)} = \frac{(10.0 - C_{\text{HCl}}) \cdot 0.020}{W_{\text{qCell}}} \quad (1)$$

where  $C_{\text{HCl}}$  is the concentration of HCl solution in which the quaternized cellulose beads were immersed (mM),  $W_{\text{qCell}}$  the weight of the quaternized cellulose beads (g). The quantity of 10.0 and 0.020 are the initial concentration (mM) and volume of HCl solution (L), respectively.

### 2.4. FT-IR and XPS Analysis

The FT-IR spectra of the untreated cellulose beads and the quaternized cellulose beads were measured by a JASCO FT/IR-4100 spectrometer. The spectra were recorded by cumulating 16 scans at the resolution of  $4.0 \text{ cm}^{-1}$ .

The XPS high-resolution spectra of  $\text{C}_{1s}$ ,  $\text{O}_{1s}$ , and  $\text{N}_{1s}$  of the untreated cellulose beads and the quaternized cellulose beads were recorded on a Shimadzu ESCA 3400 X-ray photoelectron spectrometer (Kyoto, Japan) with MgK $\alpha$  (1253.6 eV) source operated at 8 kV and 20 mA. The binding energy was calibrated with the aid of the reference to the  $\text{Au}_{4f}^{7/2}$  peak at 83.8 eV.

### 2.5. Particle Size Distribution

The photographs of the untreated cellulose beads and quaternized cellulose beads with different contents of quaternary ammonium groups in the dry and water-swollen states were taken at the magnification of 150 times through a Keyence VH-5500 microscope (Osaka, Japan). The diameter of 200 pieces of the untreated cellulose beads and the quaternized cellulose beads was measured, regarding them as a sphere, and the average size was calculated from the particle size distribution.

### 2.6. Water Absorptivity

Accurately weighed 0.05 g of the quaternized cellulose beads were immersed in water for at least 12 h at 25 °C and their weight was measured. The water content was calculated using Equation (2),

$$\text{water content (\%)} = \frac{W_{\text{wet}} - W_{\text{dry}}}{W_{\text{wet}}} \cdot 100 \quad (2)$$

where  $W_{\text{dry}}$  and  $W_{\text{wet}}$  are the weight of quaternized cellulose beads in the dry and water-swollen states.

### 2.7. Preparation of HA Solutions

About 0.125 g of HA was added to about 450 mL of water and the mixture was stirred for at least 12 h to dissolve HA. The insoluble components were removed with a filter paper, and then the filtrate was filled up to 500 mL with water. The weight concentration of the stock HA solution was determined by subtracting the weight of insoluble residues retained on the filter paper from the weight of added HA [24]. This solution was diluted with water to give the concentration from 40 to 150 mg/L, the pH value of which was adjusted to 3–12 with HCl or NaOH. The calibration curve was prepared by measuring the absorbance of HA solutions at 254 nm. A linear relationship was obtained between the absorbance and the HA concentration at this wavelength with a high regression coefficient ( $\epsilon = 12.58 \text{ dm}^3/\text{g}\cdot\text{cm}$ ,  $r = 0.9999$ ). In a preliminary experiment, it was confirmed that this

wavelength was an isosbestic point at which the adsorption coefficient remained constant in the pH range between 5 and 12. The calibration curves at 254 nm were individually prepared at other pH values.

### 2.8. Adsorption of HA

The adsorption of HA was initiated by adding a given amount of quaternized cellulose beads to the HA solutions, the pH value of which was beforehand adjusted to a predetermined one, in batch system. The experimental conditions were varied, including the initial pH value, the temperature, the dose of quaternized cellulose beads, the content of quaternary ammonium groups, and the HA concentration. Unless otherwise stated, the adsorption experiments were performed by adding 10 mg of the quaternized cellulose beads to 50 mL of a 100 mg/L HA solution at pH 3.0 or 6.0 and 25 °C. The solutions were mildly stirred and the absorbance at 254 nm was measured at predetermined time intervals until the adsorption equilibrium. The amount of adsorbed HA at time  $t$  was calculated using Equation (3),

$$\text{amount of adsorbed HA (mg/g)} = \frac{(C_0 - C_t) \cdot 0.050}{W_q} \quad (3)$$

where  $C_0$  and  $C_t$  are the concentration of HA at time 0 and  $t$ , respectively.  $W_q$  is the weight of the quaternized cellulose beads added to the HA solutions (g). The quantity of 0.050 is the volume of a HA solution (L). In addition, the removal % value was calculated from the initial and final concentrations using Equation (4).

$$\text{removal \%} = \frac{C_0 - C_{eq}}{C_0} \cdot 100 \quad (4)$$

### 2.9. Kinetic and Isothermal Analysis

The adsorption data under different conditions were analyzed by the pseudo-first and pseudo-second order models [26–32]. The pseudo-first order equation is generally expressed by

$$\ln (Q_{eq} - Q_t) = \ln Q_{eq} - k_1 t \quad (5)$$

where  $Q_t$  and  $Q_{eq}$  denote the adsorbed amount at time  $t$  and at equilibrium, respectively, and  $k_1$  is the pseudo-first order rate constant [27,28].

On the other hand, the pseudo-second order equation is expressed as

$$\frac{t}{Q_t} = \frac{t}{k_2 \cdot Q_{eq}^2} + \frac{1}{Q_{eq}} t \quad (6)$$

where  $k_2$  is the pseudo-second order rate constant [27–29].

The adsorption capacity obtained in the range of the initial HA concentrations of 0.060–0.150 mg/L was applied to Langmuir and Freundlich isotherm models represented by Equations (7) and (8), respectively [28,31].

$$\frac{C_{eq}}{Q_{eq}} = \frac{1}{K_L \cdot Q_{max}} + \frac{C_{eq}}{Q_{max}} \quad (7)$$

where  $C_{eq}$  is the HA concentration at equilibrium,  $Q_{max}$  the maximum adsorption capacity, and  $K_L$  the Langmuir adsorption constant related to the affinity of binding sites [32].

$$\log Q_{eq} = \log K_F + \frac{1}{n} \log C_{eq} \quad (8)$$

where  $K_F$  is the Freundlich constant related to adsorption capacity and  $1/n$  the empirical parameter corresponding to adsorption intensity, depending on the heterogeneity of the adsorbents [33].

### 2.10. Desorption

NaOH solutions at 10–200 mM were prepared as an eluent for desorption of HA [26]. The quaternized cellulose beads HA-loaded were immersed in the NaOH solutions at 25 °C. The absorbance at 254 nm was measured at predetermined intervals and the desorbed amount was calculated from the HA concentration in the NaOH solutions. The desorption % value was obtained from the ratio of the desorbed amount to the adsorbed amount.

## 3. Results and Discussion

### 3.1. Preparation of Quaternized Cellulose

The quaternization of cellulose beads was performed by varying the concentration of GTMAC and the reaction time. The content of quaternary ammonium groups introduced to the cellulose beads with GTMAC was determined by the back titration with HCl. The amount of HCl consumed was directly proportional to the dose of quaternized cellulose beads added to the HCl solution. Therefore, the content of quaternary ammonium groups introduced to the cellulose beads was determined from the slope of the straight line obtained (Figure S1). The content of quaternary ammonium groups of the other quaternized cellulose beads was also determined in the same manner. Since an epoxy group is involved in a nucleophilic ring-opening reaction and the reaction is fast, the content of quaternary ammonium groups was readily controlled by varying the GTMAC concentration rather than the reaction time. Figure 1 shows the change in the content of quaternary ammonium groups introduced to the cellulose beads with the concentration of GTMAC for the reaction time of 2 h at 65 °C. The content of quaternary ammonium groups increased with an increase in the concentration of GTMAC and then reached up to 0.524 mmol/g at 1.0 M.

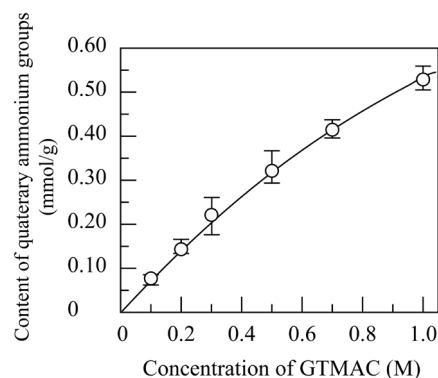


**Figure 1.** Change in the content of quaternary ammonium groups introduced to the cellulose beads with the concentration of GTMAC at the reaction time of 2 h.

In other studies, the quaternization of cellulose has been performed with GTMAC [27–29] or 3-chloro-2-hydroxypropyltrimethylammonium chloride (CHPTAC) [30,31] in the presence of NaOH. For the quaternization with CHPTAC, NaCl is generated in converting a 3-chloro-2-hydroxypropyl group of CHPTAC into an epoxypropyl group. On the other hand, when GTMAC is used in place of CHPTAC, the addition reaction of an epoxypropyl group with an OH group or a CH<sub>2</sub>OH group will occur without forming any byproduct [23,32–37]. Therefore, in this study, GTMAC was used for quaternization of the cellulose beads.

### 3.2. FT-IR and XPS Analysis

The FT-IR spectra were shown in Figure S2 for the untreated cellulose beads and the quaternized cellulose beads with the content of quaternary ammonium groups of 0.231 mmol/g. The band attributed to methyl groups of quaternary ammonium groups at 1476 cm<sup>-1</sup> and the band 1406 cm<sup>-1</sup> [37–39]. The XPS spectra of the quaternized cellulose beads were also measured, because the difference in the FT-IR spectra was small.

The XPS high-resolution spectra of  $C_{1s}$ ,  $O_{1s}$ , and  $N_{1s}$  were shown in Figure 2 for the untreated cellulose beads and the quaternized cellulose beads with 0.231 mmol/g. For the untreated cellulose beads, a peak at 286.5 eV assigned to  $-C-OH$  and  $-CH_2-OH$  and a peak at 285.0 eV assigned to  $-CH_2-CH_2-$  were observed in the  $C_{1s}$  high-resolution spectrum. An  $O_{1s}$  peak assigned to  $-OH$  also emerged at 532.7 eV. Subsequently, when the cellulose beads were quaternized with GTMAC, an  $N_{1s}$  peak assigned to  $-N^+(CH_3)_3$  groups emerged at 402.7 eV. Since the position of  $N_{1s}$  peak assigned to quaternary ammonium groups was slightly higher than those of the  $N_{1s}$  peaks assigned to amino groups and their protonated forms at about 399–402 eV, the  $N_{1s}$  peak at 402.7 eV was characteristic of a quaternary ammonium group [36,40]. As described here, the analysis by XPS emphasized that quaternary ammonium groups were successfully introduced to the cellulose beads with GTMAC according to the reaction shown in Scheme 1.

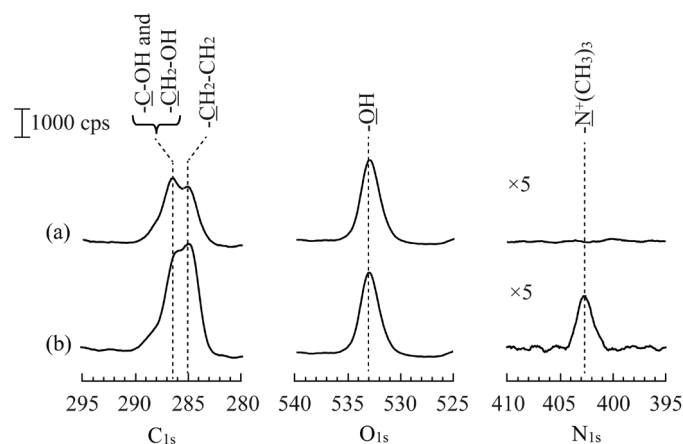
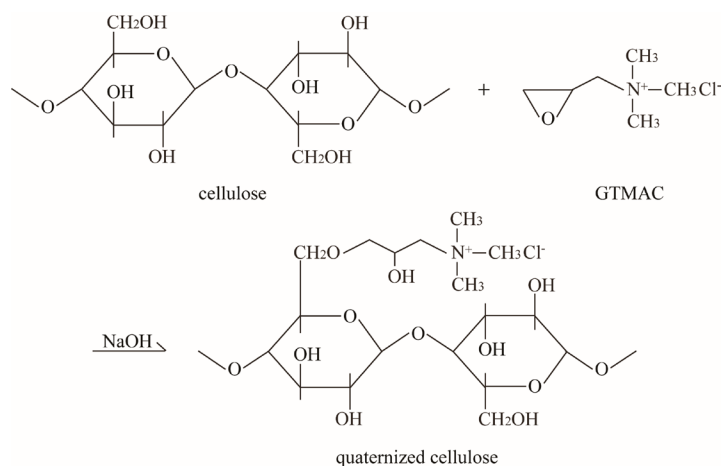


**Figure 2.** The XPS high-resolution spectra of  $C_{1s}$ ,  $O_{1s}$ , and  $N_{1s}$  for (a) the untreated cellulose beads and (b) the quaternized cellulose beads with 0.231 mmol/g.



**Scheme 1.** The schematic representation of the quaternization of cellulose beads with GTMAC.

### 3.3. Water Absorptivity

The water content of quaternized cellulose beads with different contents of quaternary ammonium groups was measured at 25 °C. The change in the water content with the content of quaternary ammonium groups is shown in Figure 3. The water content of the used cellulose beads was 81.6% and gradually increased with the content of quaternary ammonium groups. However, the water content remained unchanged in the range higher than 0.25 mmol/g. The particle size distributions of the used cellulose beads and some quaternized cellulose beads in the dry and water-swollen states are summarized in Table 1 (also see Figure S3).

The average particle size of the used cellulose beads was 0.298 mm (SD = 0.0462 mm) and 0.395 mm (SD = 0.0475 mm) in their dry and water-swollen states, respectively. As shown in Table 1, the average particle size remained almost unchanged in the dry and water-swollen states, even when the content of quaternary ammonium groups increased.

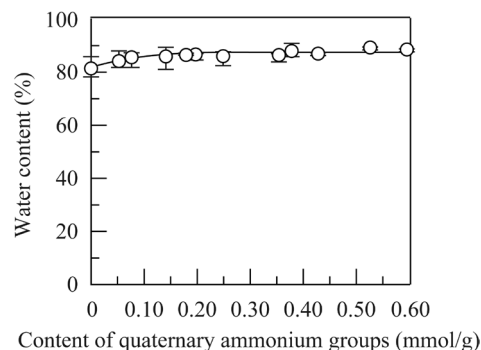


**Figure 3.** Change in the water content with the content of quaternary ammonium groups at 25 °C.

**Table 1.** The average particle sizes of the untreated and quaternized cellulose beads with different contents of quaternary ammonium groups in the dry and water-swollen states.

Content of Quaternary Ammonium Groups (mmol/g)	Untreated	0.053	0.231	0.380	0.524
in the dry state					
Average size (mm)	0.298	0.299	0.293	0.302	0.294
Standard deviation (mm)	0.046	0.050	0.048	0.041	0.038
in the water swollen state					
Average size (mm)	0.395	0.394	0.393	0.405	0.399
Standard deviation (mm)	0.048	0.049	0.050	0.045	0.037

### 3.4. HA Adsorption

#### 3.4.1. The pH Dependence

The effects of the pH value and temperature on the adsorption of HA were investigated with the quaternized cellulose beads with 0.231 mmol/g. Figure 4a shows the changes in the adsorption capacity and removal % value with the initial pH value. The adsorption capacity sharply decreased in the range of pH 4–5, and then gradually decreased with a further increase in the initial pH value. During the adsorption process, the pH value of HA solution changed, as shown in Figure 4b. A similar pH dependence has also been discussed in other articles on HA adsorption [41,42]. Figure 5 shows the change in the adsorption capacity with the pH value at equilibrium. The pH dependence of the HA adsorption will be also discussed in more detail in the Section 3.4.5.

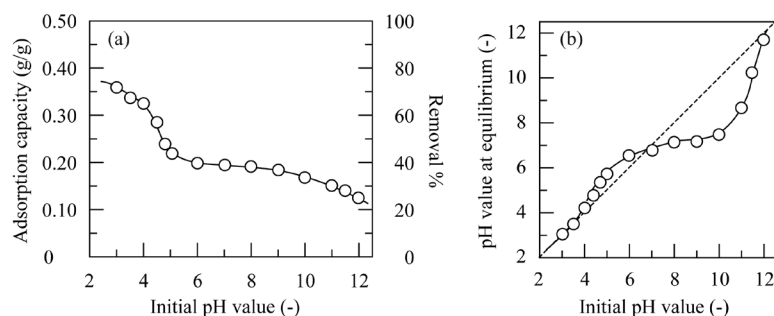


**Figure 4.** Changes in the (a) adsorption capacity and removal % value and (b) the pH value at equilibrium with the initial pH value for adsorption on the quaternized cellulose beads with 0.231 mmol/g in a 100 mg/L HA solution at 25 °C.

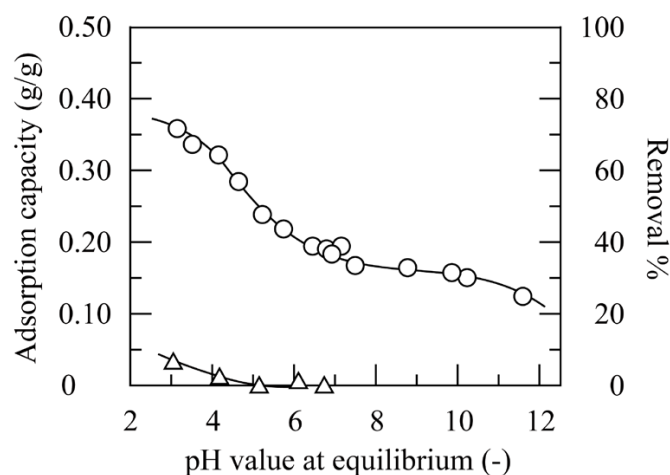


**Figure 5.** Change in the adsorption capacity and removal % value with the pH value at equilibrium for adsorption of the quaternized cellulose beads with 0.231 mmol/g in an aqueous 100 mg/L HA solution at 25 °C.

### 3.4.2. The Temperature Dependence

The temperature dependence of the HA adsorption was assessed at pH 3 and 6. Figure 6 shows the changes in the adsorption capacity and  $k_2$  value with the temperature. Although the adsorption capacity was almost constant against the temperature, the  $k_2$  value obtained from the pseudo-second order reaction equation increased with an increase in the temperature. The fit to the pseudo-second order model of HA adsorption will be also discussed in the Section 3.4.5. A linear relationship was obtained between the reciprocal of temperature and the  $\ln k_2$  value. The activation energy calculated from the slopes of the straight lines was 14.5 and 36.3 kJ/mol at pH 3 and 6, respectively. In general, the adsorption process can be categorized into the physical and chemical adsorptions by the magnitude of activation energy. It is said that the specificity and involvement of strong forces characteristic of chemical adsorption require more than 4.2 kJ/mol of activation energy [42,43]. Therefore, the above-mentioned values suggest that the adsorption in this study occurred through the chemical reaction. In addition, a low activation energy at pH 3.0 supports that the HA adsorption more successfully proceeded at this pH value as shown in Figures 4 and 5.

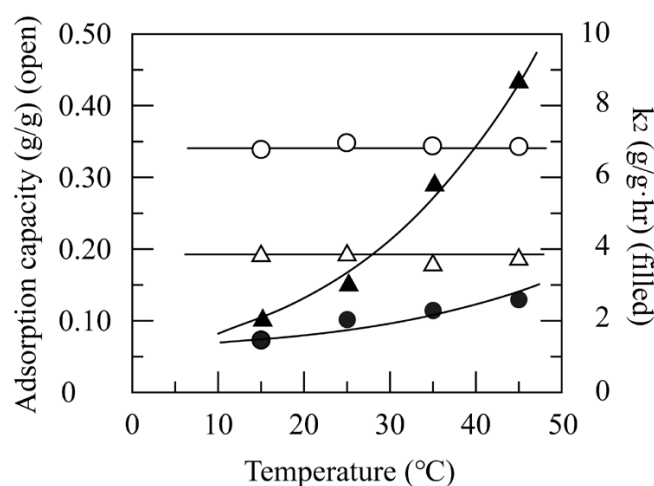
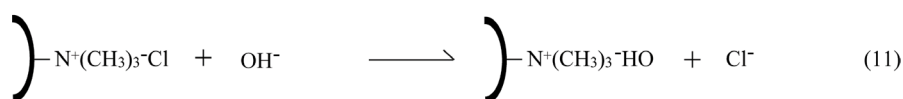
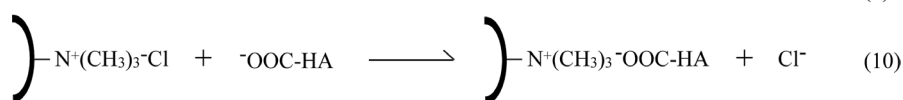
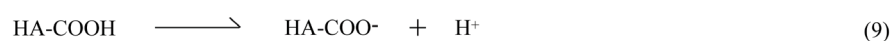


**Figure 6.** Changes in the adsorption capacity (open) and  $k_2$  value (filled) with the temperature for adsorption on the quaternized cellulose beads with 0.231 mmol/g in an aqueous 100 mg/L HA solution at pH 3.0 (○,●) and 6.0 (△,▲).

Based on the results obtained above, the interaction involved in the adsorption of HA on the quaternized cellulose beads will be discussed. First of all, HA is a macromolecular compound with two or more than negatively chargeable functional groups, such as carboxy groups and phenolic hydroxy groups. The presence of these functional groups contributes to the acidity of HA, although the number of these functional groups depends on the source of origin as well as the conditions of extraction and production processes [44,45]. A high adsorption capacity was obtained at pH 3–4, as shown in Figures 4 and 5, contrary to our expectations, in spite of the fact that only some of the HA molecules present in the solution were in the anionic form at pH 3–4. HA is successfully adsorbed on the quaternized cellulose beads through the interaction, or ion exchange reaction, between a dissociated carboxy group of a HA molecule and a quaternary ammonium group of the quaternized cellulose beads according to Equation (10) in Scheme 2 [34]. This reaction led to the decrease in the concentration of dissociated carboxy groups in the outer solution, and consequently the dissociation of carboxy groups of HA molecules was promoted (see Equation (9) in Scheme 2).



**Scheme 2.** The schematic representation of the proposed mechanism of the adsorption of HA molecules on the quaternized cellulose beads.

Subsequently, the decrease in the adsorption capacity will be discussed. The molecular size of HA in water increases at higher pH values due to the intramolecular electrostatic repulsion between dissociated carboxy groups [46]. The ion repulsion between dissociated carboxy groups in HA molecules binding to the quaternized cellulose beads and ones of HA molecules present in the outer solution probably inhibits the adsorption of HA molecules [47]. In addition, hydroxide ions added in the HA solution to adjust the pH value are a competition ion of carboxy ions. Therefore, the increase in the concentration of hydroxide ions also leads to the decrease in the adsorption capacity in the range of pH values higher than 7. As a whole, the multiple involvement of the above-mentioned factors results in the decrease in the adsorption capacity [48].

### 3.4.3. The Content of Quaternary Ammonium Groups

At 25 °C, 10 mg of quaternized cellulose beads with different contents of quaternary ammonium groups were added to HA solutions of pH 3.0 and 6.0. Figure 7 shows the changes in the adsorption capacity and removal % value with the content of quaternary ammonium groups. The adsorption capacity increased with an increase in the content of quaternary ammonium groups and the adsorption capacity at pH 3.0 was higher than that at pH 6.0 irrespective of the content of quaternary ammonium groups. In particular, at pH 6.0, the adsorption capacity was directly proportional to the content of quaternary ammonium groups below 0.231 mmol/g, and then deviated from the straight line at further increased contents of quaternary ammonium groups. In addition, the adsorption capacity of 0.036 was obtained at pH 3.0 for the untreated cellulose beads. This suggests that hydrogen bonding between undissociated carboxy or phenolic hydroxy groups of a HA molecule and alcoholic hydroxy groups of cellulose beads or generated through the addition reaction with GTMAC would have also been involved in adsorption of HA. The removal % value went up to 86.1% at pH 3.0 and 61.7% at pH 6.0 for the quaternized cellulose beads with 0.524 mmol/g.

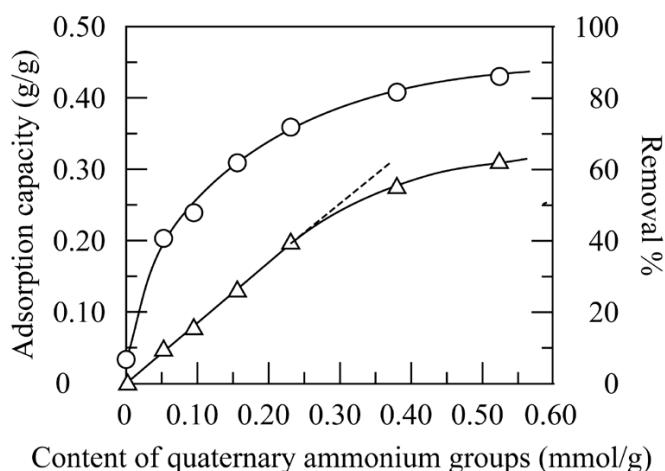


**Figure 7.** Changes in the adsorption capacity and removal % value with the content of quaternary ammonium groups at pH 3.0 (○) and 6.0 (△).

### 3.4.4. The Dose of Quaternized Cellulose Beads

Different doses of quaternized cellulose beads with 0.231 mmol/g were added to HA solutions to increase the removal of HA. Figure 8 shows the changes in the adsorption capacity and removal % value with the dose of quaternized cellulose beads at pH 3.0 and 6.0. The adsorption capacity decreased and the removal % value increased with the increase in the dose of quaternized cellulose beads at pH 3.0. On the other hand, at pH 6.0, the removal % value was directly proportional to the dose of quaternized cellulose beads, and the adsorption capacity was constant in the range below 20 mg (dose = 0.40 g/L), and then the adsorption capacity gradually decreased at further increased doses of quaternized cellulose beads. This would have been caused mainly by the fact that HA adsorption progressively occurred, and the HA concentration sharply decreased. The removal % value reached over 90% by addition of 30 mg (dose = 0.60 g/L) at pH 3.0 and by addition of 40 mg (dose = 0.80 g/L) at pH 6.0. This indicates that HA was highly removed from the outer solution through the adsorption process.

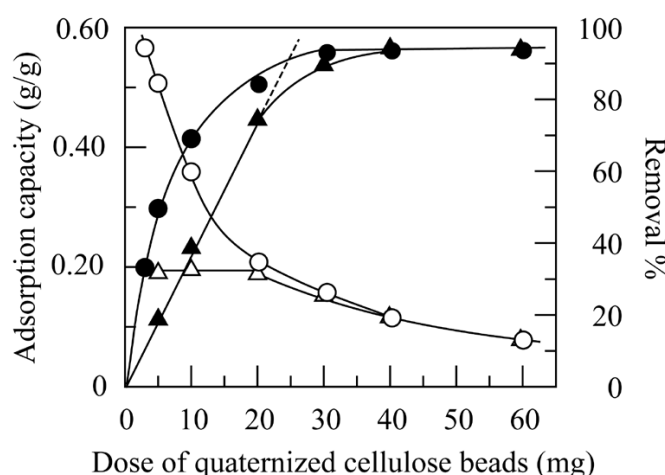


**Figure 8.** Changes in the adsorption capacity (open) and removal % value (filled) with the dose of quaternized cellulose beads at pH 3.0 (○,●) and 6.0 (△,▲).

### 3.4.5. Kinetic Analysis

The kinetic parameters calculated by the pseudo first-order and second-order equations were summarized in Table 2 for HA adsorption on the quaternized cellulose beads

with 0.231 mmol/g at pH 3.0, 6.0, and 9.0 as typical results. A typical example of the kinetic analysis is shown in Figure S4. The kinetic data fit to the pseudo-first order model only for initial short immersion times, although the theoretically estimated values of the adsorption capacity obtained from the intercept were close to the experimental values. On the other hand, the adsorption processes followed the pseudo-second order model with correlation coefficients higher than 0.99 for 7–8 h and the theoretically estimated values of the adsorption capacity obtained from the slope were quite close to the experimental values with the small relative errors. As shown in Figure 9, the  $k_2$  value gradually increased with an increase in the pH value and had the maximum value at pH 6–7. The increase in  $k_2$  value is attributed to the fact that although the adsorption capacity decreased with an increase in the pH value as shown in Figure 5, the rate of adsorption was higher at higher pH values. The time course of HA adsorption at pH 3 and 6 is shown in Figure S5. However, at further increased pH values, the increase in the hydroxy ion concentration resulted in the decrease in the rate of adsorption and adsorption capacity. As compared with the results shown in Figure 6, the pH value also influenced the  $k_2$  value, although it was to a much lesser extent than the temperature. To be specific, the adsorption of HA occurred through the electrostatic interaction of a quaternary ammonium group introduced to the cellulose beads with a dissociated carboxy group affixed to a HA molecule as shown in Scheme 2.

**Table 2.** The kinetic parameters calculated by the pseudo first-order and second-order equations for the quaternized cellulose beads with 0.231 mmol/g at pH 3.0, 6.0 and 9.0.

pH	$Q_{exp}$ (g/g)	$Q_{cal}$ (g/g)	Relative Error (%)	$k_1$ (1/h)	$r^2$ (–)	Time Range (min)
3	0.359	0.35	–2.36	1.667	0.9088	5
6	0.195	0.192	–1.49	0.504	0.9952	40
9	0.195	0.187	–4.09	1.253	0.9938	5
pH	$Q_{exp}$ (g/g)	$Q_{cal}$ (g/g)	Relative Error (%)	$k_2$ (g/g·h)	$r^2$ (–)	Time Range (h)
3	0.359	0.355	–1.14	2.288	0.9988	7
6	0.195	0.194	–0.55	3.072	0.9996	8
9	0.195	0.199	1.99	2.943	0.995	7

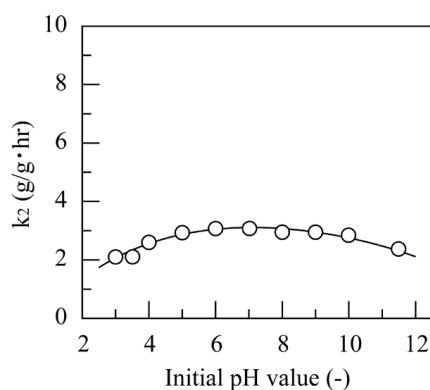


**Figure 9.** Change in the  $k_2$  value with the initial pH value for the quaternized cellulose beads with 0.231 mmol/g.

### 3.4.6. Analysis by Langmuir and Freundlich Adsorption Isotherms

On the basis of the fact that HA adsorption fit to the pseudo-second order model, the adsorption capacity at different concentrations was analyzed by the isotherms to provide the qualitative information. The adsorption capacity was determined in the range of the initial HA concentrations of 0.060–0.150 mg/L at pH 3.0 and 6.0 for the quaternized cellulose

beads with 0.231 mmol/g and applied to Langmuir and Freundlich isotherm models [28,31]. The Langmuir and Freundlich parameters are summarized in Table 3. Figure S6 shows the linear forms of (a) Langmuir and (b) Freundlich isotherms. The Langmuir isotherm model fit better with a little higher regression coefficient than the Freundlich isotherm model. The fit to Langmuir isotherm indicates that the HA adsorption will proceed with an assumption of a 1:1 ratio between an active site, a quaternary ammonium group, and a dissociated carboxy group of a HA molecule as adsorbate. The calculated  $Q_{max}$  values in Table 3 were much higher than the experimental  $Q_{eq}$  values shown in Figure 5, which suggests that the quaternized cellulose beads prepared in this study have a high potential to adsorb HA molecules. The calculated  $Q_{max}$  value at pH 3.0 was higher than that at pH 6.0. This suggests that the decrease in the adsorption capacity would have been caused mainly by the ionic repulsion between HA molecules and the accompanying increase in the size of HA molecules. In addition, the  $K_L$  value at pH 3.0 was higher than that at pH 6.0. Since the Langmuir constant is a measure of the affinity of an adsorbate to an adsorption site, the  $K_L$  value at pH 3.0 also supports successful adsorption of HA on the quaternized cellulose beads at this pH value.

**Table 3.** The Langmuir and Freundlich parameters for HA adsorption on the quaternized cellulose beads with 0.231 mmol/g at pH 3.0 and 6.0.

Langmuir Isotherm			Freundlich Isotherm		
$Q_{max}$ (g/g)	pH 3.0 0.775	pH 6.0 0.378	n	pH 3.0 1.86	pH 6.0 2.17
$K_L$ (dm <sup>3</sup> /mg)	0.0313	0.0174	$K_F$ (mg/g)/(dm <sup>3</sup> /mg) <sup>1/n</sup>	0.0548	0.0288
$r^2$	0.9895	0.9996	$r^2$	0.9866	0.9925

### 3.5. Comparison with Other Adsorbents

The adsorption capacities obtained by other adsorbents for HA removal were summarized in Table 4 to compare with ours [2,3,24,26,42,49–56]. However, we should bear in mind in advance that it is difficult to directly compare our adsorption capacity with others, since the experimental conditions, such as the initial pH value, temperature, concentration and volume of HA solution, and dose of adsorbent, vary from article to article. However, it was found that among articles on polymeric adsorbent used for removal of HA, the adsorption capacity obtained in this study was considerably higher than those of other adsorbents, which should be specially mentioned. This emphasizes that the quaternized cellulose beads prepared in this study have a high potentiality as an adsorbent for removal of HA.

**Table 4.** The comparison with HA adsorption capacities of adsorbents reported in other articles.

Adsorbent	pH	Temp. (°C)	HA Conc. (mg/L)	Dose (g/L)	Q (mg/g)	Ref.
quaternized cellulose beads	3.0	25	100	0.20	359	this study
cetylpyridium bromide modified zeolite	7.5	30	60	0.40	92	[2]
amine-modified PAAM-bentonite composite	6	50	167.5	2.00	82.6	[3]
quaternized cellulose fibers	6	room temp.	500	0.50	310	[24]
magnetic Fe <sub>3</sub> O <sub>4</sub> @SiO <sub>2</sub> -PANI particle	6	25	41.85	0.50	36.36	[26]
PEI-modified fungal biomass	5	25	100	1.00	41.5	[42]
Fe <sub>3</sub> O <sub>4</sub> @Na-BP-PEI particles	6.7	20	91	0.20	114	[49]
PDMAEMA/pumice stone hydrogel composite	4	20	50	0.50	59.72	[50]
amine-modified silica aerogel	5	35	250	1.00	236.4	[51]
PEI modified magnetic graphite	4	20	21	0.25	83.71	[52]
quaternized DMAEMA grafted cotton linter	6	30	800	1.00	333.3	[53]
PAAm/chitosan semi IPN hydrogel	7	25	80	0.50	148.7	[54]
chitosan/cellulose acetate-cellulose nanocrystal fibers	4.0	25	30	0.06	151.4	[55]
electrospun cellulose acetate/chitosan fibers	4.0	25	30	0.04	184.7	[56]

### 3.6. Desorption

The economic feasibility of the adsorption process is dealt with the regeneration of the used adsorbents in practical applications. The HA desorption was investigated by immersing the quaternized cellulose beads with 0.231 mmol/g loaded with HA in NaOH solutions at different concentrations at 25 °C. The quaternized cellulose beads had the average amount of adsorbed HA of 0.166 (0.156–0.177) mg/g by immersing in the HA solutions for 16 h at pH 6.0. Figure 10 shows the changes in the desorption % and desorption time with the NaOH concentration at 25 °C. The desorption % value increased with an increase in the NaOH concentration and HA was almost completely released from the quaternized cellulose beads for 100 min and the quaternized cellulose beads were decolorized from deep green to white at 100 mM. In addition, when the NaOH concentration was further increased, the desorption time was shortened. After the desorption, the quaternized cellulose beads were treated with pH 3 HCl solution. Then, when immersed in a HA solution at pH 6 again, the adsorbed amount of 0.168 mg/g was obtained. This value was quite close to that of the first run (0.177 mg/g). These results indicate that the quaternized cellulose beads were regenerated and could be reused for HA removal. The regeneration of the used adsorbents is crucial for industrial and large-scale practical applications. This will reduce the operational cost of the process as well as minimize the ecological risk factor, or secondary pollution.

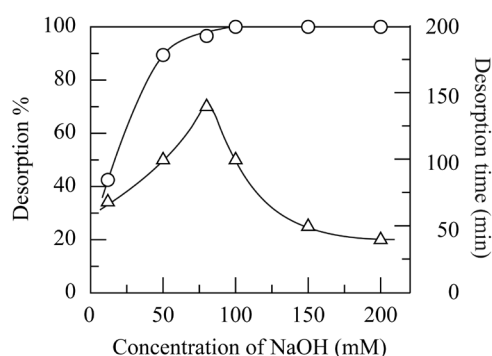


**Figure 10.** Changes in the desorption % value (○) and desorption time (△) with the concentration of NaOH at 25 °C.

## 4. Conclusions

In this study, the cellulose beads were quaternized with GTMAC in the presence of NaOH and the HA adsorption of the resulting quaternized cellulose beads was investigated by varying the experimental conditions, such as the pH value, the temperature, the content of quaternary ammonium groups, and the dose of quaternized cellulose beads. In addition, the kinetic, isothermal, and thermodynamic properties of HA adsorption were analyzed for their application as a promising adsorbent.

The content of quaternary ammonium groups was controlled with changing the GTMAC concentration. The introduction of quaternary ammonium groups to the cellulose beads was confirmed by FT-IR and XPS analysis and the content of quaternary ammonium groups determined by the back titration with HCl increased to higher than 0.5 mmol/g. The adsorption capacity of the quaternized cellulose beads increased with a decrease in the pH value and the maximum adsorption capacity was obtained at pH 3.0. On the other hand, although the adsorption capacity remained unchanged against the temperature, the  $k_2$  value obtained from the pseudo-second order equation increased with an increase in the temperature. The kinetics of HA adsorption obeyed the pseudo-second order model and the adsorption capacity at different concentrations was well described by the Langmuir isotherm. These results emphasize that the HA adsorption will occur through the chemical bonding (interaction) between adsorbates and functional groups on the surfaces of the adsorbents, or the electrostatic interaction between a quaternary ammonium group on

the quaternized cellulose beads and a dissociated carboxy group of a HA molecule. The removal % value increased with the increase in the content of quaternary ammonium groups and the dose of quaternized cellulose beads. The removal % value reached over 90% by addition of 30 mg (dose = 0.60 g/L) at pH 3.0 and by addition of 40 mg (dose = 0.80 g/L) at pH 6.0 for the quaternized cellulose beads with 0.231 mmol/g, indicating that HA was almost completely removed from the aqueous medium. The adsorption capacity obtained in this study was compatible to or higher than those of other articles. It should be noted that the adsorbent with excellent adsorption performance for removal of HA was constructed from porous cellulose beads through the quaternization. In addition, the results obtained in this study demonstrated that the quaternized cellulose beads are an effective and economically viable adsorbent for removal of HA. However, for practical applications, further studies should be conducted in the mixed and multi-pollutants system and in the presence of salt to satisfy the requirements of wastewater treatment.

**Supplementary Materials:** The following supporting information can be downloaded at: <https://www.mdpi.com/article/10.3390/physchem3010005/s1>, Figure S1: The determination of the content of quaternary ammonium groups by the back titration with HCl for the quaternized cellulose beads with the content of quaternary ammonium groups of 0.231 mmol/g; Figure S2: The FT-IR spectra of (a) the untreated cellulose beads and (b) the quaternized cellulose beads with 0.231 mmol/g. Figure S3: The particle distributions of the untreated cellulose beads in the (a) dry and (b) water-swollen states; Figure S4: The kinetic analysis of the time source of HA adsorption on the quaternized cellulose beads at the content of quaternary ammonium groups of 0.231 mmol/g by the (a) pseudo first- and (b) second-order equations; Figure S5: The time course of HA adsorption on the quaternized cellulose beads at the content of quaternary ammonium groups of 0.231 mmol/g at pH 3.0 (○) and 6.0 (△); Figure S6: The linear forms of (a) Langmuir and (b) Freundlich isotherms for the HA adsorption on the quaternized cellulose beads at the content of quaternary ammonium groups of 0.231 mmol/g at pH 3.0 (○) and 6.0 (△).

**Author Contributions:** Conceptualization, H.M. and K.Y.; methodology, H.A., H.M. and K.Y.; validation, H.A. and K.Y.; investigation, K.U.; resources, K.Y.; data curation, K.U. and K.Y.; writing—original draft preparation, K.Y.; writing—review and editing, H.A., H.M. and K.Y.; visualization, K.U. and K.Y.; supervision, K.Y.; project administration, K.Y. All authors have read and agreed to the published version of the manuscript.

**Funding:** This research received no external funding.

**Institutional Review Board Statement:** Not applicable.

**Informed Consent Statement:** Not applicable.

**Data Availability Statement:** All the data are available within the manuscript.

**Conflicts of Interest:** The authors declare no conflict of interest.

## References

1. Klučáková, M.; Pelikán, P.; Lapčík, L.; Lapčíková, B.; Kučerík, J.; Kaláb, M. Structure and properties of humic and fulvic acids. 1. Properties and reactivity of humic acids and fulvic acids. *J. Polym. Mater.* **2000**, *17*, 337–356.
2. Zhan, Y.; Zhu, Z.; Lin, J.; Qiu, Y.; Zhao, J. Removal of humic acid from aqueous solution by cetylpyridinium bromide modified zeolite. *J. Environ. Sci.* **2010**, *22*, 1327–1334. [[CrossRef](#)] [[PubMed](#)]
3. Anirudhan, T.S.; Suchithra, P.S.; Rijith, S. Amine-modified polyacrylamide-bentonite composite for the adsorption of humic acid in aqueous solutions. *Colloids Surf. A Physicochem. Eng. Asp.* **2008**, *326*, 147–156. [[CrossRef](#)]
4. De Melo, B.A.G.; Motta, F.L.; Santana, M.H.A. Humic acids: Structural properties and multiple functionalities for novel technological developments. *Mater. Sci. Eng. C.* **2016**, *62*, 967–974. [[CrossRef](#)] [[PubMed](#)]
5. Murbach, T.S.; Glávits, R.; Endres, J.R.; Clewell, A.E.; Hirka, G.; Vértési, A.; Szakonyiné, I.P. A toxicological evaluation of a fulvic and humic acids preparation. *Toxicol. Rep.* **2020**, *7*, 1242–1254. [[CrossRef](#)]
6. Zhang, X.; Ding, Z.; Yang, J.; Cizmas, L.; Lichtfouse, E.; Sharma, V.K. Efficient microwave degradation of humic acids in water using persulfate and activated carbon. *Environ. Chem. Lett.* **2018**, *16*, 1069–1075. [[CrossRef](#)]
7. Zhu, X.; Liu, J.; Li, L.; Zhen, G.; Lu, X.; Zhang, J.; Liu, H.; Zhou, Z.; Wu, Z.; Zhang, X. Prospects for humic acids treatment and recovery in wastewater: A review. *Chemosphere* **2023**, *312*, 137193. [[CrossRef](#)]
8. Wall, N.A.; Choppin, G.R. Humic acids coagulation: Influence of divalent cations. *Appl. Geochem.* **2003**, *18*, 1573–1582. [[CrossRef](#)]

9. Lowe, J.; Hossain, M.M. Application of ultrafiltration membranes for removal of humic acid from drinking water. *Desalination* **2008**, *218*, 343–354. [[CrossRef](#)]
10. Doskočil, L.; Grasset, L.; Válková, D.; Pakař, M. Hydrogen peroxide oxidation of humic acids and lignite. *Fuel* **2014**, *134*, 406–413. [[CrossRef](#)]
11. Wen, P.; Liu, D.; Chen, W.; Jiang, G.; Li, Q. Decomposition of humic acid by ozone: Oxidation properties and water-matrix constituents. *Desalination Water Treat.* **2020**, *174*, 98–105. [[CrossRef](#)]
12. Islam, M.A.; Morton, D.W.; Johnson, B.B.; Angove, M. Adsorption of humic and fulvic acids onto a range of adsorbents in aqueous systems, and their effect on the adsorption of other species: A review. *Sep. Purif. Technol.* **2020**, *247*, 116949. [[CrossRef](#)]
13. Kołodziej, A.; Fuentes, M.; Baigorri, R.; Lorenc-Brabowska, E.; García-Mina, J.M.; Burg, P.; Gryglewicz, G. Mechanism of adsorption of different humic acid fractions on mesoporous activated carbons with basic surface characteristics. *Adsorption* **2014**, *20*, 667–675. [[CrossRef](#)]
14. Eustáquio, H.M.B.; Lopes, C.W.; da Rocha, R.S.; Cardoso, B.D.; Pergher, S.B.C. Modification of activated carbon for the adsorption of humic acid. *Adsorpt. Sci. Technol.* **2015**, *33*, 117–126. [[CrossRef](#)]
15. Habuta-stanić, M.; Tutić, A.; Grgić, D.K.; Zeko-Pivač, A.; Burilo, A.; Paixão, S.; Teixeira, V.; Pagaimo, M.; Pala, A.; Ravančić, M.E.; et al. Adsorption of humic acid from water using chemically modified bituminous coal-based activated carbons. *Chem. Biochem. Eng. Q.* **2021**, *35*, 189–203. [[CrossRef](#)]
16. Klemm, D.; Heublein, B.; Fink, H.P.; Bohn, A. Cellulose: Fascinating biopolymer and sustainable raw material. *Angew. Chem. Int. Ed.* **2005**, *44*, 3358–3393. [[CrossRef](#)]
17. Hokkanen, S.; Bhatnagar, A.; Sillanpää, M. A review on modification methods to cellulose-based adsorbents to improve adsorption capacity. *Water Res.* **2016**, *91*, 156–173. [[CrossRef](#)]
18. Wohler, M.; Bensefelt, T.; Wågberg, L.; Furó, I.; Berglund, L.A.; Wohler, J. Cellulose and the role of hydrogen bonds: Not in charge of everything. *Cellulose* **2022**, *29*, 1–23. [[CrossRef](#)]
19. Peng, B.; Yao, Z.; Wang, X.; Crombeen, M.; Sweeney, D.G.; Tam, K.C. Cellulose-based materials in wastewater treatment of petroleum industry. *Green Energy Environ.* **2020**, *5*, 37–49. [[CrossRef](#)]
20. Rana, A.K.; Mishra, Y.K.; Gupta, V.K.; Thakur, V.K. Sustainable materials in the removal of pesticides from contaminated water: Perspective on macro to nanoscale cellulose. *Sci. Total Environ.* **2021**, *797*, 149129. [[CrossRef](#)]
21. Kaur, J.; Sengupta, P.; Mukhopadhyay, S. Critical review of bioadsorption on modified cellulose and removal of divalent heavy metals (Cd, Pb, and Cu). *Ind. Eng. Chem. Res.* **2022**, *61*, 1921–1954. [[CrossRef](#)]
22. Abdelhamid, H.N.; Mathew, A.P. Cellulose-based materials for water remediation: Adsorption, catalysis, and antifouling. *Front. Chem. Eng.* **2021**, *3*, 790314. [[CrossRef](#)]
23. Kopač, T.; Krajnc, M.; Ručigaj, A. A rheological study of cationic micro- and nanofibrillated cellulose: Quaternization reaction optimization and fibril characteristic effects. *Cellulose* **2022**, *29*, 1435–1450. [[CrossRef](#)]
24. Sehaqui, H.; de Larraya, U.P.; Tingaut, P.; Zimmermann, T. Humic acid adsorption onto cationic cellulose nanofibers for bioinspired removal of copper (II) and a positively charged dye. *Soft Matter* **2015**, *11*, 5294–5300. [[CrossRef](#)] [[PubMed](#)]
25. Sehaqui, H.; Mautner, A.; de Larraya, U.P.; Pfenninger, N.; Tingaut, P.; Zimmermann, T. Cationic cellulose nanofibers from waste pulp residues and their nitrate, fluoride, sulphate and phosphate adsorption properties. *Carbohydr. Polym.* **2016**, *135*, 334–340. [[CrossRef](#)]
26. Nishino, A.; Taki, A.; Asamoto, H.; Minamisawa, H.; Yamada, K. Kinetic, isotherm, and equilibrium investigation of Cr (VI) ion adsorption on amine-functionalized porous silica beads. *Polymers* **2022**, *14*, 2104. [[CrossRef](#)]
27. Saha, B.; Orvig, C. Biosorbents for hexavalent chromium elimination from industrial and municipal effluents. *Coord. Chem. Rev.* **2010**, *254*, 2959–2972. [[CrossRef](#)]
28. Parlayici, S.; Pehlivan, E. Comparative study of Cr(VI) removal by bio-waste adsorbents: Equilibrium, kinetics, and thermodynamic. *J. Anal. Sci. Technol.* **2019**, *10*, 15. [[CrossRef](#)]
29. Ho, Y. Second-order kinetic model for the sorption of cadmium onto tree fern: A comparison of linear and non-linear methods. *Water Res.* **2006**, *40*, 119–125. [[CrossRef](#)]
30. Ho, Y. Review of second-order models for adsorption systems. *J. Hazard. Mater.* **2006**, *B136*, 681–689. [[CrossRef](#)]
31. Foo, K.Y.; Hameed, B.H. Insights into the modeling of adsorption isotherm systems. *Chem. Eng. J.* **2010**, *156*, 2–10. [[CrossRef](#)]
32. Langmuir, I. The adsorption of gases on plane surfaces of glass, mica and platinum. *J. Am. Chem. Soc.* **1918**, *40*, 1361–1403. [[CrossRef](#)]
33. Freundlich, H. Über die Adsorption in Lösungen. *Zeit. Phys. Chem.* **1907**, *57*, 385–470. [[CrossRef](#)]
34. Wang, J.; Bi, L.; Ji, Y.; Ma, H.; Yin, X. Removal of humic acid from aqueous solution by magnetically separable polyaniline: Adsorption behavior and mechanism. *J. Colloid Interface Sci.* **2014**, *430*, 140–146. [[CrossRef](#)]
35. Courtenay, J.C.; Hohns, M.A.; Galembeck, F.; Deneke, C.; Lanzoni, E.M.; Costa, C.A.; Scott, J.L.; Sharma, R.I. Surface modified cellulose scaffolds for tissue engineering. *Cellulose* **2017**, *24*, 253–267. [[CrossRef](#)] [[PubMed](#)]
36. Udoetok, I.A.; Wilson, L.D.; Headley, J.V. Quaternized cellulose hydrogels as sorbent materials and pickering emulsion stabilizing agents. *Materials* **2016**, *9*, 645. [[CrossRef](#)]
37. Quinlan, P.J.; Tanvir, A.; Tam, K.C. Application of the central composite design to study the flocculation of an anionic azo dye using quaternized cellulose nanofibrils. *Carbohydr. Polym.* **2015**, *133*, 80–89. [[CrossRef](#)]

38. Zhang, H.; Guo, H.; Wang, B.; Shi, S.; Xiong, L.; Chen, X. Synthesis and characterization of quaternized bacterial cellulose prepared in homogeneous aqueous solution. *Carbohydr. Polym.* **2016**, *136*, 171–176. [[CrossRef](#)]
39. Song, Y.; Sun, Y.; Zhang, X.; Zhou, J.; Zhang, L. Homogeneous quaternization of cellulose in NaOH/urea aqueous solutions as gene carriers. *Biomacromolecules* **2008**, *9*, 2259–2264. [[CrossRef](#)]
40. Yamada, K.; Kitao, K.; Asamoto, H.; Minamisawa, H. Development of recoverable adsorbents for Cr(VI) ions by grafting of a dimethylamino group-containing monomer on polyethylene substrate and subsequent quaternization. *Environ. Technol.* **2021**. [[CrossRef](#)]
41. Deng, S.; Bai, R. Adsorption and desorption of humic acid on aminated polyacrylonitrile fibers. *J. Colloid Interface Sci.* **2004**, *280*, 36–43. [[CrossRef](#)]
42. Deng, S.; Yu, G.; Ting, Y. Removal of humic acid using PEI-modified fungal biomass. *Separat. Sci. Technol.* **2006**, *41*, 2989–3002. [[CrossRef](#)]
43. Manirethan, V.; Raval, K.; Rajan, R.; Thaira, H.; Balakrishnan, R.M. Kinetic and thermodynamic studies on the adsorption of heavy metals from aqueous solution by melanin nanopigment obtained from marine source: *Pseudomonas stutzeri*. *J. Environ. Manag.* **2018**, *214*, 315–324. [[CrossRef](#)] [[PubMed](#)]
44. Rupiasih, N.N.; Vidyasagar, P.B. A review: Compositions, structures, properties and applications of humic substances. *J. Adv. Sci. Technol.* **2005**, *8*, 16–25.
45. Sánchez-Monedero, M.A.; Cegarra, J.; García, D.; Roig, A. Chemical and structural evolution of humic acids during organic waste composting. *Biodegradation* **2002**, *13*, 361–371. [[CrossRef](#)]
46. Avena, M.J.; Koopal, L.K. Kinetics of humic acid adsorption at solid-water interfaces. *Environ. Sci. Technol.* **1999**, *33*, 2739–2744. [[CrossRef](#)]
47. Bousba, S.; Bougdah, N.; Messikh, N.; Magri, P. Adsorption removal of humic acid from water using a modified Algerian bentonite. *Phys. Chem. Res.* **2018**, *6*, 613–625.
48. Zularisam, A.W.; Ismail, A.F.; Salim, R. Behaviours of natural organic matter in membrane filtration for surface water treatment—A review. *Desalination* **2006**, *194*, 211–231. [[CrossRef](#)]
49. Zhang, J.; Ning, F.; Kang, M.; Ma, C.; Qiu, Z. Effective removal of humic acid from aqueous solution using adsorbents prepared from the modified waste bamboo powder. *Microchem. J.* **2020**, *153*, 104272. [[CrossRef](#)]
50. Taktak, F.; Ibay, Z. Synthesis of novel poly[2-(dimethylamino) ethyl methacrylate]/pumice stone hydrogel composite for the rapid adsorption of humic acid in aqueous solution. *J. Macromol. Sci. A Pure Appl. Chem.* **2015**, *52*, 307–315. [[CrossRef](#)]
51. Chen, K.; Feng, Q.; Feng, Y.; Ma, D.; Wang, D.; Liu, Z.; Zhu, W.; Li, X.; Qin, F.; Feng, J. Ultrafast removal of humic acid by amine-modified silica aerogel: Insights from experiments and density functional theory calculation. *Chem. Eng. J.* **2022**, *435*, 135171. [[CrossRef](#)]
52. Zhang, J.; Kang, M.; Zhou, Y.; Ma, C.; Ning, F.; Qiu, Z. Facile synthesis of polyethyleneimine modified magnetic graphite: An effective adsorbent for the removal of humic acid from aqueous solution. *Mater. Chem. Phys.* **2020**, *255*, 123549. [[CrossRef](#)]
53. Du, J.; Dong, Z.; Pi, Y.; Yang, X.; Zhao, L. Fabrication of cotton linter-based adsorbents by radiation grafting polymerization for humic acid removal from aqueous solution. *Polymers* **2019**, *11*, 962. [[CrossRef](#)]
54. Liu, Z.; Zhou, S. Removal of humic acid from aqueous solution using polyacrylamide/chitosan semi-IPN hydrogel. *Water Sci. Technol.* **2018**, *2017*, 16–26. [[CrossRef](#)]
55. Zhang, Y.; Wang, Y. Electrospun cellulose-acetate/chitosan fibers for humic-acid removal: Improved efficiency and robustness with a core-sheath design. *Nanomaterials* **2022**, *12*, 1284. [[CrossRef](#)]
56. Zhang, Y.; Wang, F.; Yixiang, W. Electrospun cellulose acetate/chitosan fibers for humic acid removal: Construction guided by intermolecular interaction study. *Appl. Polym. Mater.* **2021**, *3*, 5022–5029. [[CrossRef](#)]

**Disclaimer/Publisher’s Note:** The statements, opinions and data contained in all publications are solely those of the individual author(s) and contributor(s) and not of MDPI and/or the editor(s). MDPI and/or the editor(s) disclaim responsibility for any injury to people or property resulting from any ideas, methods, instructions or products referred to in the content.